International Journal of Nanomedicine

Dovepress

open access to scientific and medical research

Open Access Full Text Article

ORIGINAL RESEARCH

Red Blood Cell-Hitchhiking Delivery of Simvastatin to Relieve Acute Respiratory Distress Syndrome

Mengjuan Sun[1,*], Jun Wei[1,*], Yanhui Su[1,*], Yangjingwan He[1], Liang Ge[1], Yan Shen[1], Bohui Xu[2], Yanlong Bi[3], Chunli Zheng[1]

[1]Department of Pharmaceutics, China Pharmaceutical University, Nanjing, People's Republic of China; [2]School of Pharmacy, Nantong University, Nantong, People's Republic of China; [3]Pediatric Intensive Care Unit, Children's Hospital of Nanjing Medical University, Nanjing, People's Republic of China

*These authors contributed equally to this work

Correspondence: Chunli Zheng; Yanlong Bi, Email zhengchunli@cpu.edu.cn; pulong123@163.com

Purpose: The purpose of this study is to address the high mortality and poor prognosis associated with Acute Respiratory Distress Syndrome (ARDS), conditions characterized by acute and progressive respiratory failure. The primary goal was to prolong drug circulation time, increase drug accumulation in the lungs, and minimize drug-related side effects.

Methods: Simvastatin (SIM) was used as the model drug in this study. Employing a red blood cell surface-loaded nanoparticle drug delivery technique, pH-responsive cationic nanoparticles loaded with SIM were non-covalently adsorbed onto the surface of red blood cells (RBC), creating a novel drug delivery system (RBC@SIM-PEI-PPNPs).

Results: The RBC@SIM-PEI-PPNPs delivery system effectively extended the drug's circulation time, providing an extended therapeutic window. Additionally, this method substantially improved the targeted accumulation of SIM in lung tissues, thereby enhancing the drug's efficacy in treating ARDS and impeding its progression to ARDS. Crucially, the system showed a reduced risk of adverse drug reactions.

Conclusion: RBC@SIM-PEI-PPNPs demonstrates promise in ARDS and ARDS treatment. This innovative approach successfully overcomes the limitations associated with SIM's poor solubility and low bioavailability, resulting in improved therapeutic outcomes and fewer drug-related side effects. This research holds significant clinical implications and highlights its potential for broader application in drug delivery and lung disease treatment.

Keywords: acute lung injury, simvastatin, respiratory distress syndrome, pH response

Introduction

Acute Respiratory Distress Syndrome (ARDS), which are characterized by inflammatory lung damage due to various direct or non-cardiogenic lung injuries.[1–3] The mechanisms behind ARDS involve the activation of alveolar macrophages and type II epithelial cells, leading to the release of inflammatory and chemotactic factors, resulting in a cascade of inflammation.[4,5] The current treatment strategy for ARDS is mainly supportive treatment, mainly including Lung-protective ventilation strategies (LPVS), stem cell therapy, glucocorticoids,[6–8] surfactants,[9] and N-acetyl cysteine Amino acids,[10–12] statins,[13–15] neutrophil elastase inhibitors[16-18] and other drug intervention treatments. However, no effective strategy for treating ARDS has been found so far, and the mortality rate of patients with ARDS is still as high as 30~50%.[19,20] An effective treatment system for ARDS needs further research.[21]

Simvastatin (SIM) is widely used to treat hypercholesterolemia and cardiovascular diseases. Recent research has revealed that SIM has multiple biological activities and pharmacological effects beyond cholesterol reduction, including anti-inflammatory,[22,23] anti-fibrotic, immunomodulatory,[24] anti-tumor,[25,26] and antioxidant properties. This multifaceted pharmacological profile positions SIM as a promising candidate for the treatment of ARDS. Several studies have reported the beneficial effects of high-dose SIM in various animal models of lung injury, showcasing its potential to protect the lungs. However, a significant challenge with SIM is its high binding affinity to plasma proteins, with approximately 95% of SIM

Received: 22 January 2024
Accepted: 22 May 2024
Published: 6 June 2024

extensively undergoing first-pass hepatic absorption, resulting in low bioavailability (less than 5%).[27] Furthermore, due to physiological barriers in the lungs, systemic administration of SIM has limited lung-specific drug delivery efficiency, potentially causing systemic side effects and restricting its clinical application. Therefore, Targeted delivery and enhanced bioavailability of anti-inflammatory agents to local sites of inflammation are promising strategies for disease treatment. In recent years, biomimetic nano-delivery systems based on cell membranes have attracted more and more attention.[28] Meanwhile, mature mammalian RBC have a distinctive biconcave elliptical shape, lack a cell nucleus and many organelles, and possess a relatively simple structure. They offer several advantages as drug carriers compared to synthetic drug delivery systems, including low immunogenicity, a large surface area for drug loading, and prolonged circulation time,[29–32] Nanoparticles coated with membranes from platelets were developed to target damaged blood vessels or sites of inflammation in the lungs because platelets have an intrinsic affinity for sites of inflammation.[33]

Based on the low pH value of the ARDS inflammatory microenvironment (IME),[34] to better deliver the SIM to the lungs, this study employs poly (lactic-co-glycolic acid) (PLGA) as a carrier material, polyethyleneimine (PEI) as a cationic agent, and SIM as the model drug. Sodium bicarbonate ($NaHCO_3$) serves as the pH-responsive factor. By using these components, pH-responsive cationic PLGA nanoparticles are synthesized to enhance SIM bioavailability. In the low pH environment of ARDS, high concentrations of hydronium ions (H_3O^+) react with $NaHCO_3$ in the PLGA nanoparticles' shell to produce CO_2 and H_2O, leading to the breakdown of the PLGA nanoparticle shell and the burst release of the drug. These positively charged pH-responsive PLGA nanoparticles nonspecifically adsorb to the surface of red blood cells with high efficiency and remain in circulation for an extended period. This approach constructs a red blood cell-loaded SIM pH-responsive cationic PLGA nanoparticle drug delivery system. When administered through intravenous injection in ALI mice, the SIM-loaded pH-responsive cationic PLGA nanoparticles target the lung capillary endothelium, potentially translocating into the lung alveolar Inflammatory microenvironment. In the low pH environment of lung inflammation, SIM is released from the nanoparticles, thereby achieving the therapeutic effect.

Materials and Methods

Materials

Simvastatin (Anhui Zesheng Technology Co., Ltd.), Polyvinyl Alcohol 1788 (PVA) (China National Pharmaceutical Group Chemical Reagent Co., Ltd.), Poly(lactic-co-glycolic acid) (PLGA, 50:50, 15,000 Da) (Shandong Medical Device Research Institute), Dichloromethane (Shanghai Lingfeng Chemical Reagent Co., Ltd.), Sodium Bicarbonate (Shanghai Meilin Biochemical Technology Co., Ltd.), Polyethyleneimine (PEI, 10,000 Da) (Shanghai Aladdin Reagent Co., Ltd.), Glucose (China National Pharmaceutical Group Chemical Reagent Co., Ltd.), Mannitol (China National Pharmaceutical Group Chemical Reagent Co., Ltd.), Sucrose (China National Pharmaceutical Group Chemical Reagent Co., Ltd.). All experiments were conducted according to the guidelines of experimental animals and approved by the regional Ethics Committee of China Pharmaceutical University (ethics approval number: 202,202,018).

Preparation of Simvastatin pH-Responsive Cationic Nanoparticles (SIM-PEI-PPNPs)

Precisely weigh SIM (5 mg) and PLGA (25 mg) into an EP tube, add 1 mL of dichloromethane, and vortex until completely dissolved to form the oil phase. Precisely weigh a certain amount of $NaHCO_3$ and dissolve it in a 1% PVA aqueous solution to create the inner aqueous phase (The concentration of $NaHCO_3$ was 5 mg/mL). Precisely weigh PVA 100 mg, add it to deionized water 10 mL, and heat while stirring until completely dissolved. Adjust the solution's pH to neutral after adding an appropriate 25 mg of PEI to create the outer aqueous phase. Subsequently, pH-responsive nanoparticles with surface-adsorbed PEI-carrying SIM are prepared using an emulsion solvent evaporation method. Take 200 μL of the inner aqueous phase and add it to the oil phase. Under ice bath conditions at 4°C, use an ultrasound probe at 100 W power (1 s on, 2 s off) for 30s to form the primary emulsion. While magnetic stirring, add the primary emulsion dropwise to the outer water phase. Under ice bath conditions at 4°C, use an ultrasound probe at 100 W power (1 s on, 2 s off) for 150 s to obtain a milky white secondary emulsion. Place this secondary emulsion under reduced pressure and rotate-evaporate it at 37°C for 30 min until dichloromethane is completely evaporated, resulting in a pale blue colloidal suspension of nanoparticles. Freeze-dry, set aside.

Characterization of SIM-PEI-PPNPs

Morphological Study of SIM-PEI-PPNPs

A 30 μL aliquot of the diluted nanoparticle solution was dropped onto a copper grid and allowed to settle for 10 min. Excess liquid on the surface of the copper grid was absorbed using filter paper. The grid was then stained with a 2% phosphotungstic acid solution for 2 min. The copper grid was placed under an infrared lamp and dried for 10 min, after which the morphology of the nanoparticles was observed and photographed under a transmission electron microscope (Hitachi Japan Co., Ltd., HT-7700).

Stability Assessment of SIM-PEI-PPNPs

The prepared SIM-PEI-PPNPs were stored in the dark at 4°C. Samples were taken at 0, 1, 3, 5, and 7 days to measure using a Zetasizer Nano-ZS90 (Malvern Instruments, UK), observing any changes to assess their stability during storage.

Particle Size and Zeta Potential Measurement

A 100 μL aliquot of the nanoparticles was drawn using a micro-pipette and diluted to an appropriate multiple with deionized water. Particle size and Zeta potential were determined using a Zetasizer Nano-ZS90 (Malvern Instruments, UK).

SIM-PEI-PPNPs Release in vitro

Transfer 1 mL of SIM-PEI-PPNPs colloidal suspension into a dialysis bag and immerse it in 50 mL of phosphate buffer solution containing 30% ethanol (pH 6.5 or pH 7.4) as the release medium. Place the dialysis bag in a 37°C, 120 rpm constant-temperature shaker. At various time points (0.5, 1, 2, 4, 6, 8, 12, 24 h), withdraw 1 mL of the release medium and store it in a 4°C refrigerator. Simultaneously, replenish with an equal volume of fresh release medium at the same temperature. The drug content in the filtered release medium from different time points was determined using HPLC, and the cumulative drug release was calculated to generate in vitro release profiles. The cumulative release rates at each sampling point were calculated according to formula (2), and release curves for SIM-PEI-PPNPs in different pH release media were plotted.

$$Q_n = \frac{(C_1 + C_2 + C_3 + C_4 + \ldots + C_{n-1}) * V_1 + C_n * V_2}{C_0 * V_0} * 100\% \quad (1)$$

Where: Q_n is the cumulative release rate at each time point. C_n is the SIM concentration at each time point. C_0 is the initial concentration of SIM. V_1 is the sampling volume at each instance. V_2 is the total volume of the release medium. V_0 is the initial volume into which SIM-PEI-PPNPs were introduced.

Collection of Red Blood Cells

In fresh whole blood from SD rats, add a large volume of ice-cold PBS (more than 10 times the blood volume). Centrifuge at 4°C and 1300 rpm for 6 min in a low-temperature high-speed centrifuge. Remove the supernatant and collect the red precipitate. Subsequently, wash it with ice-cold PBS two to three times until the supernatant is no longer visibly red, effectively removing platelets, plasma, white blood cells, and other components from the blood. The resulting precipitate is the packed red blood cells (RBC) after PBS washing.

Preparation of RBC@SIM-PEI-PPNPs

Weigh an appropriate amount of freeze-dried SIM-PEI-PPNPs powder with precision and place it in an EP tube. Add isotonic PBS and vortex until complete dissolution, resulting in a nano-particle suspension of SIM-PEI-PPNPs with a concentration of 1 mg/mL, characterized by a pale blue opalescence. Take a specific volume of the nano-particle suspension and combine it with 50 μL of packed red blood cells in a 1.5 mL centrifuge tube. Add isotonic PBS to reach a total volume of 1 mL, and gently mix by repeatedly pipetting for 3–4 min. Incubate at 37°C for 30 min. Following incubation, wash the mixture three times with ice-cold PBS at 4°C and 100 g for 5 min to remove any unbound nanoparticles, resulting in the formation of RBC@SIM-PEI-PPNPs.

Red Blood Cell-Related Toxicity Studies

Red Blood Cell Aggregation Study

Add 50, 100, 200, 300, and 400 μL of 1 mg/mL SIM-PEI-PPNPs suspension to 50 μL of red blood cells for the preparation of RBC@SIM-PEI-PPNPs. Disperse RBC@SIM-PEI-PPNPs in an isotonic PBS solution to create a suspension for the study of red blood cell aggregation. Take 80 μL of the RBC@SIM-PEI-PPNPs suspension and add it to the U-shaped wells of a 96-well organic glass blood coagulation plate. Incubate at room temperature for 1 h, using blank red blood cell suspension as a negative control for red blood cell aggregation. Investigate the impact of adding SIM-PEI-PPNPs/RBC (w/v) concentrations of 1, 2, 4, 6, and 8 mg/mL on the aggregation of red blood cell carriers.

Red Blood Cell Hemolysis Study

Take the supernatant obtained after centrifuging 50, 100, 200, 300, and 400 μL of 1 mg/mL SIM-PEI-PPNPs suspension with 50 μL of red blood cells and transfer it to a 5 mL volumetric flask. Dilute with purified water to the mark and shake well. Take an equal volume of red blood cells and add purified water and isotonic PBS as negative and positive controls, respectively. Dilute the supernatant with an appropriate amount of purified water. Use a UV-visible spectrophotometer to measure the absorbance of hemoglobin in the supernatant at 540 nm. Assess the hemolysis of red blood cell carriers prepared with SIM-PEI-PPNPs/RBC (w/v) concentrations of 1, 2, 4, 6, and 8 mg/mL. Calculate the hemolysis percentage (%)[35] using the formula (3).

$$Hemolysie\,(\%) = \frac{OD_t - OD_{nc}}{OD_{pc} - OD_{nc}} \tag{2}$$

Where *ODt* represents the absorbance of the experimental sample solution, *ODnc* represents the absorbance of the negative control solution, and *ODpc* represents the absorbance of the positive control solution.

Characterization of RBC@SIM-PEI-PPNPs

Scanning Electron Microscopy (SEM)

The morphology of RBC@SIM-PEI-PPNPs was observed using SEM. 50 μL of the freshly prepared RBC@SIM-PEI-PPNPs sample was placed in a 1.5 mL Eppendorf tube, and a 2.5% cold glutaraldehyde fixative solution (4°C) was slowly added along the tube wall. The tube was stored in a refrigerator at 4°C overnight. After discarding the fixative solution, the sample was rinsed three times with 0.1 M pH 7.0 phosphate buffer, each time for 15 min. Subsequently, the sample was fixed with a 1% osmium tetroxide solution, and after removing the osmium tetroxide, it was rinsed three more times with 0.1 M pH 7.0 phosphate buffer. The sample was then dehydrated sequentially with 30%, 50%, 70%, 80%, 90%, and 95% ethanol solutions, each for 15 min, followed by two treatments with 100% ethanol, each for 20 min. The sample was then treated with a mixture of ethanol and isoamyl acetate (v/v = 1/1) for 30 min, and subsequently with pure isoamyl acetate for 1 h. The sample was then dried and coated in a critical point dryer, and the prepared sample was observed and analyzed for the morphology of the red blood cell carriers using a scanning electron microscope.

Flow Cytometry Analysis

C6-labeled nanoparticles were co-incubated with freshly prepared red blood cells to prepare RBC@C6-PEI-PPNPs. The mixture was centrifuged and washed three times to remove any free nanoparticles. The mixture was then diluted with isotonic PBS to achieve a cell concentration of 1×10^6 cells/mL. Blank red blood cells served as a negative control. Flow cytometry was used to measure the fluorescence intensity of nanoparticles on the surface of RBC@C6-PEI-PPNPs and to quantitatively determine the number of red blood cells with surface-bound fluorescently labeled nanoparticles.

Determination of Zeta Potential

An appropriate dilution of blank red blood cells and freshly prepared RBC@SIM-PEI-PPNPs in isotonic PBS was prepared. 0.7 mL of the diluted suspensions of blank red blood cells and red blood cells loaded with the drug system were taken, and their Zeta potential values were measured using a Zetasizer Nano-ZS90 (Malvern Instruments, UK).

Encapsulation Efficiency Determination

The prepared nanoparticle colloidal suspension was filtered through a 0.22 μm microfiltration membrane to remove free drug crystals. A suitable volume of the filtered nanoparticle colloidal suspension was then subjected to centrifugation at 16,000 rpm and 4°C for 40 min to eliminate any remaining free drug in the supernatant. The resulting precipitate was ultrasonically disrupted in the mobile phase for 10 min, and the drug content within the nanoparticles was measured, denoted as W_1. An equal volume of undisturbed drug-loaded nanoparticle colloidal suspension, which had not been filtered through the membrane, was taken. It was also subjected to ultrasonic disruption in the mobile phase for 10 min to determine the total drug content, labeled as W_2. Encapsulation efficiency of the nanoparticles was calculated using the formula (1)

$$EE\% = \frac{W_1}{W_2} \times 100\% \tag{3}$$

Evaluation of RBC@SIM-PEI-PPNPs in vitro

Osmotic Fragility Assessment

Osmotic fragility testing is used to assess the ability of red blood cell membranes to withstand changes in osmotic pressure within a medium. Hemolysis rates (%) of both blank-packed red blood cells and RBC@SIM-PEI-PPNPs were determined by suspending them in solutions of different NaCl concentrations and examining their osmotic fragility.[36] Firstly, prepare various concentration gradients of NaCl solutions. Take 5 mL of each concentration gradient of NaCl solution and add it to a 15 mL centrifuge tube. Then, add 50 μL of freshly prepared blank-packed red blood cells and RBC@SIM-PEI-PPNPs to each tube, gently mix the red cell suspension, and allow it to stand at room temperature for 30 min. After incubation, centrifuge each set of samples at 10,000 rpm, 4°C for 10 min. Collect the supernatant and measure the ultraviolet absorbance of hemoglobin (Hb) at 540 nm using a UV spectrophotometer. Hemolysis rates are calculated relative to the ultraviolet absorbance of Hb obtained in purified water, where RBC are nearly completely lysed. Finally, plot the osmotic fragility curve.

Turbulent Fragility Test

In this test, 200 μL of freshly prepared blank-packed red blood cells and RBC@SIM-PEI-PPNPs are separately suspended in 10 mL of isotonic PBS solution. They are then agitated for 8 h at 120 rpm on a temperature-controlled shaker at 37°C. Samples (500 μL) are collected at 0, 1, 2, 3, 4, 5, 6, and 8 h, with an equivalent volume of PBS solution added simultaneously. The obtained sample solutions are diluted with PBS buffer to a total volume of 5.0 mL and then centrifuged at 3000 rpm for 5 min. The supernatant is collected, and the absorbance of hemoglobin (HB) at 540 nm is measured using a UV spectrophotometer. The absorbance of hemoglobin in isotonic PBS at 540 nm serves as the blank control, and the ultraviolet absorbance of HB obtained in purified water is taken as 100%. Hemolysis rates are calculated, and a turbulent fragility curve is plotted.

Preparation of Red Blood Cell Ghosts

Take an appropriate amount of blank-packed packed red blood cells (RBC) and place them in a 1.5 mL Eppendorf tube. Add ultrapure water and vortex until the red blood cells swell and rupture. Centrifuge the tube at 3500 rpm, 4°C for 10 min, and wash the RBC with ultrapure water three times. The resulting pellet represents the red blood cell ghosts. Subsequent detection was performed using a flow cytometer following the kit's instructions.

Shear Force Experiments in vitro

The viscosity of red blood cell PBS dispersion, which is approximately 1×103 Pa s, was utilized in accordance with Newton's law of viscosity ($\tau = \eta\gamma$) to establish shear rates of 1000 s- and 6000 s-. These shear rates were implemented using the Fluidicam microfluidic visual viscometer to replicate the shear stress encountered by red blood cells in both normal blood vessels (1 Pa) and constricted capillaries in the lungs (6 Pa).[37] Freshly prepared RBC@SIM-PEI-PPNPs, with a hematocrit of 20% and a volume of 2 mL, were dispersed in an isotonic PBS solution and exposed to these two constant shear stresses for a duration of 20 min. The shedding of nanoparticles from red blood cells was subsequently examined. Before applying shear force, 10% fetal bovine serum was added to the cell suspension to prevent the re-adhesion of shed nanoparticles.

Red Blood Cell Surface-Loaded Nanoparticle Intracellular Distribution Experiment

Preparation of pH-Responsive DiR-Loaded Nanoparticles on Red Blood Cell Surfaces

Under subdued lighting conditions, precisely weigh 2.0 mg of DiR in a 5 mL Eppendorf tube. Add 1 mL of dichloromethane and vortex until completely dissolved, creating the organic phase. Precisely weigh a certain amount of $NaHCO_3$ and dissolve it in a 1% PVA aqueous solution to form the inner aqueous phase (The concentration of $NaHCO_3$ was 5 mg/mL). Take 200 μL of the inner aqueous phase and add it to the organic phase. Using an ultrasonic probe at 4°C and a power setting of 50 W, perform sonication (1 s on, 2 s off) for 30s to form the primary emulsion. Under magnetic stirring, slowly add the primary emulsion dropwise into an outer aqueous phase containing 1% PVA and 0.2% PEI. Using an ultrasonic probe at 4°C and a power setting of 100 W, perform sonication (1 s on, 2 s off) for 100 s to obtain a milky-white secondary emulsion. This secondary emulsion is then vacuum-rotary evaporated at 37°C for 30 min until the dichloromethane has completely evaporated, resulting in a suspension of DiR pH-responsive nanoparticles (DiR-PEI-PPNPs). RBC@DiR-PEI-PPNPs were prepared like RBC@SIM-PEI-PPNPs.

Distribution Experiment in vivo

Healthy ICR mice were intravenously injected with DiR-PEI-PPNPs and RBC@DiR-PEI-PPNPs at a dose of 20 μg per mouse. After 0.5 h and 2 h, the mice were anesthetized with 3% isoflurane, and in vivo DiR (750/820 nm) fluorescence imaging was performed using an IVIS® Spectrum system. Following imaging, After the eyeball was taken with blood, the mice were euthanized, and their major organs (heart, liver, spleen, lungs, and kidneys) were collected, and washed with physiological saline, excess moisture was removed with filter paper, and the fluorescence intensity within the isolated organs and blood were observed by placing them on black cardboard. The data were processed using Living Image 4.5 software (Caliper Life Sciences, USA).

Animal Pharmacological Study of Red Blood Cell Surface-Loaded Nanoparticles

Experimental Protocol

ICR male mice were used to establish an ARDS mouse model by intratracheal instillation of 2.0 mg/mL lipopolysaccharide (LPS) in a 50 μL physiological saline solution. Mice were anesthetized, and the trachea was exposed for LPS instillation, followed by suturing the wound. The ARDS model was induced 5 h later. ICR male mice were randomly divided into 5 groups, each receiving 1.2 mg/kg of SIM through tail vein injection to evaluate the therapeutic effects of free SIM, SIM-PEI-PPNPs, and RBC@SIM-PEI-PPNPs. Treatments were initiated after tracheal LPS instillation or in control conditions. After 24 h, mice were euthanized by enucleation of the eyeball, and blood was collected. Serum was obtained after standing at room temperature for 1 h and used to measure TNF-α and IL-6 levels. Lung tissues were dissected, washed, dried, and stored at −80°C for subsequent experiments.

Lung Wet/Dry Weight Ratio Determination

The left lung of the mice was taken and washed with physiological saline. Any surface blood and excess moisture were immediately removed using filter paper. The lung tissue was placed in aluminum foil, and the wet weight (W) was recorded. The lung tissue wrapped in aluminum foil was then placed in an 80°C oven and continuously dried for 48 h until a constant weight was achieved, and the dry weight (D) was recorded. The lung wet/dry weight ratio (W/D) for each sample was calculated.

MPO Activity Assay

The right half of the lung tissue from mice was used. The surface blood was rinsed with saline, and the saline was then blotted dry with filter paper before proceeding with subsequent operations. Then the right lung tissue was placed in a frozen grinding tube. A proportional amount of physiological saline and pre-chilled grinding beads were added. A 10% weight/volume lung tissue homogenate was prepared. Low-temperature grinding was performed in a cold grinding machine (60 Hz power, running for 60s with 10s intervals, for a total of 10 cycles). Centrifugation was not required. A portion of the 10% lung tissue homogenate was taken and mixed with a two-fold concentrated reagent solution. After thorough mixing, MPO activity in the lung tissue was directly determined according to the instructions of the MPO assay kit.

Inflammatory Factor Detection of Serum and Lung Tissues

Mouse serum samples were stored at −80°C. Following the instructions of TNF-α and IL-6 ELISA assay kits, the levels of inflammatory factors TNF-α and IL-6 in the serum were measured with an ELISA kit. Furthermore, we took different groups of mouse lung tissues and measured the inflammatory factors of TNF-α and IL-6 in the lung tissues of different groups of mice with an ELISA kit.

Lung Tissue Pathological Morphological Observation

A portion of the right lung tissue from mice was placed in a 4% paraformaldehyde solution and fixed for 48 h. After paraffin embedding, 4–5 μm thick slices were prepared using a pathological slicer. These slices were then dried and subjected to H&E staining for pathological examination. Then, we performed histological evaluation of the lung tissues of different groups of mice according to the evaluation scores in Table 1.[38]

Statistical Analysis

Statistical analysis was performed using a standard Student's *t*-test and Two-Way ANOVA. *$p < 0.05$ was considered significant. **$p < 0.01$ and ***$p < 0.001$ were highly significant compared to corresponding controls. All the data were expressed as mean ± SD and at least triplicate independent experiments were carried out. Data were analyzed using Prism 8.0 software (GraphPad,La Jolla,CA).

Results

Preparation and Characterization of SIM-PEI-PPNPs

As shown in Figure 1A, SIM-PEI-PPNPs exhibit a clear and transparent appearance with a faint blue opalescent phenomenon. As shown in Figure 1B, the images revealed that the produced nanoparticles were spherical, regular in shape, possess a smooth surface, exhibit relatively uniform particle size, and display good dispersion without significant aggregation. The nanoparticle sizes observed in the transmission electron microscopy images align with those measured by the Zetasizer Nano-ZS90 (Malvern Instruments, UK). The nanoparticles show a distinct core-shell structure on their surface, indicating the successful encapsulation of the cationic polymer PEI on the nanoparticle surface.

As shown in Figure 1C, it was evident that the average particle size and PDI values of SIM-PEI-PPNPs remained stable within 7 days of preparation, signifying the excellent stability of the nanoparticles, making them suitable for long-term storage at 4°C.

Figure 1D demonstrated that the average particle size of SIM-PEI-PPNPs was 135.37 ± 0.87 nm, with a PDI of 0.085 ± 0.016, indicating small particle size, narrow and uniform distribution. The Zeta potential of SIM-PEI-PPNPs was 21.81 ± 3.65 mV, suggesting a positive surface charge and good physical stability. This also confirmed the successful surface encapsulation of PEI, reversing the nanoparticle surface from negative to positive charge.

The experimental results show that the release profile of SIM-PEI-PPNPs in vitro was depicted in Figure 1E. Under pH 7.4 conditions, SIM release was slow, with only 42.93% released within 24 h. As the pH decreases, the release amount increases, reaching an accumulated drug release of 59.27% at pH 6.5. This indicates that the prepared SIM-PEI-PPNPs exhibit pH-responsive drug release characteristics.

Characterization of RBC@SIM-PEI-PPNPs

The efficiency of adsorbing nanoparticles on the red blood cell carrier was determined to be 45.91 ± 2.53%, and the drug loading capacity was 116.50 ± 6.42 μg/mL RBC. Using SEM to observe the microstructure of RBC@SIM-PEI-PPNPs,

Table 1 Histological Scoring system

Pathological Morphology	Pulmonary edema	Infiltration of Inflammatory Cells in the Alveolar and Interstitial Spaces	Alveolar and Interstitial Hemorrhage	Atelectasis and Formation of the Hyaline Membrane
Score	1	2	3	4

Notes: Data from Lei et al.[38]

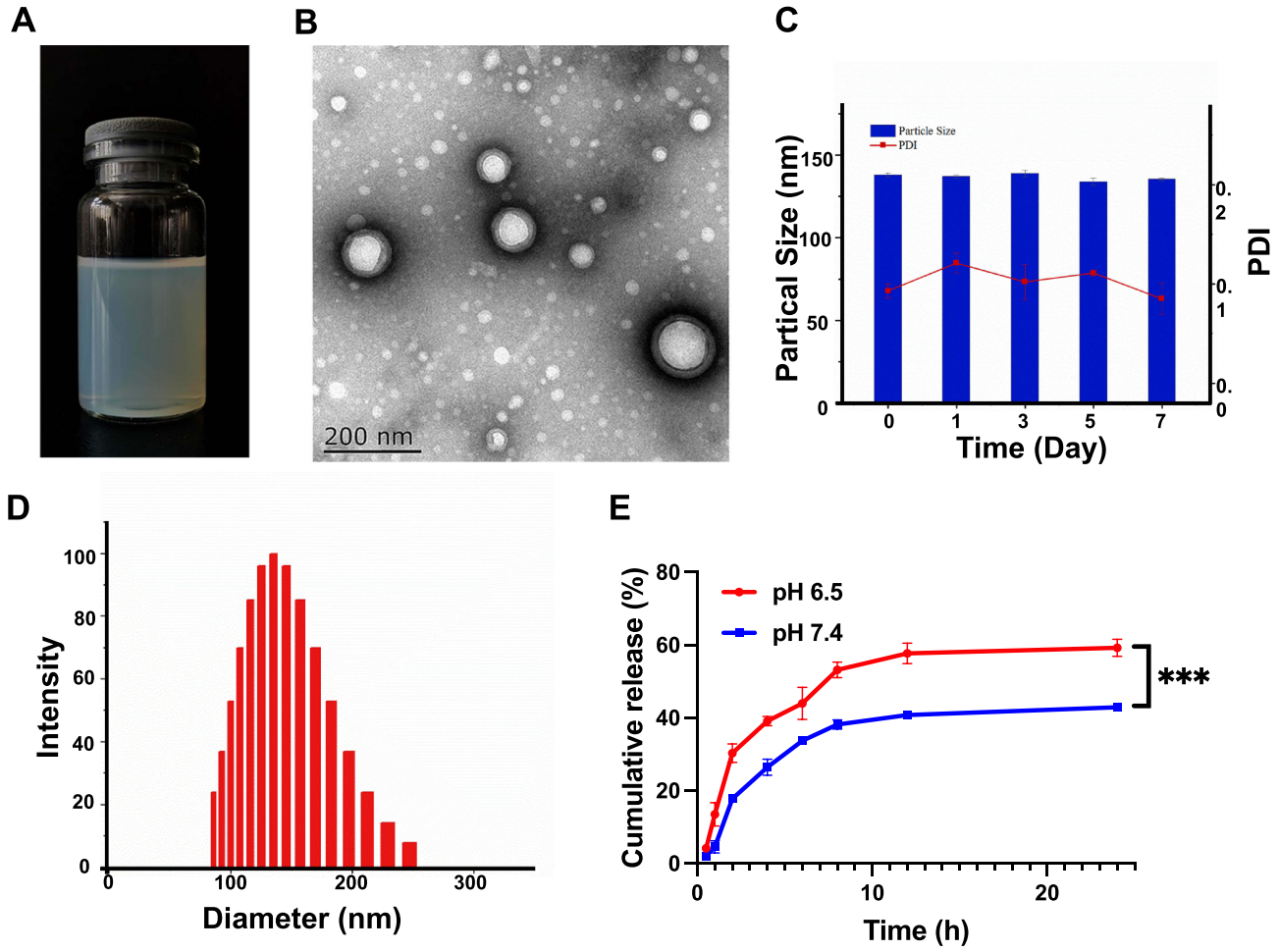

Figure 1 The characterization of SIM-PEI-PPNPs. (**A**) The appearance and (**B**) TEM image of SIM-PEI-PPNPs. Scare bare = 200 nm. (**C**) Stability of SIM-PEI-PPNPs when stored at 4°C for 7 days (n = 3). (**D**) The particle size distribution of SIM-PEI-PPNPs. (**E**) The cumulative release curves of SIM-PEI-PPNPs in pH 6.5 and pH 7.4 (n = 3, ***p < 0.001).

as shown in Figure 2A, SEM images revealed that the red blood cells exhibited a biconcave discoid shape, with spherical nanoparticles adsorbed on their surfaces. Importantly, the adsorption of nanoparticles on the red blood cell surfaces does not significantly affect the morphology of the red blood cells.

Flow cytometry analysis of RBC@C6-PEI-PPNPs prepared after co-incubation of C6-PEI-PPNPs with blank red blood cells was presented in Figure 2B. Compared to blank red blood cells, the majority of RBC@C6-PEI-PPNPs show fluorescence positivity on the red blood cell carrier surface. When the nanoparticle concentration is 6 mg/mL, the percentage of red blood cell carriers with fluorescence positivity was 99.93 ± 0.057%, indicating that approximately 99.93% of red blood cell surfaces have adsorbed nanoparticles.

The surface potential of the red blood cell carriers, both blank and loaded with nanoparticles, was assessed using a Zeta potential analyzer. As shown in Figure 2C, the results show that the Zeta potential on the surface of blank red blood cells was −13.4 ± 1.06 mV, while the Zeta potential on the surface of red blood cell carriers with adsorbed nanoparticles was −11.9 ± 0.94 mV. This may be due to the positively charged nanoparticles adsorbed on the red blood cell carrier surfaces, resulting in a slight increase in the surface potential of the red blood cell carriers themselves.

Red Blood Cell-Related Toxicity Studies

The results of red blood cell aggregation studies are illustrated in Figure 2D. When the nanoparticle concentration reaches 8 mg/mL, the red blood cell carriers exhibit an aggregation phenomenon. By reducing the nanoparticle concentration to 6 mg/mL, the aggregation effect caused by positively charged nanoparticles can be avoided.

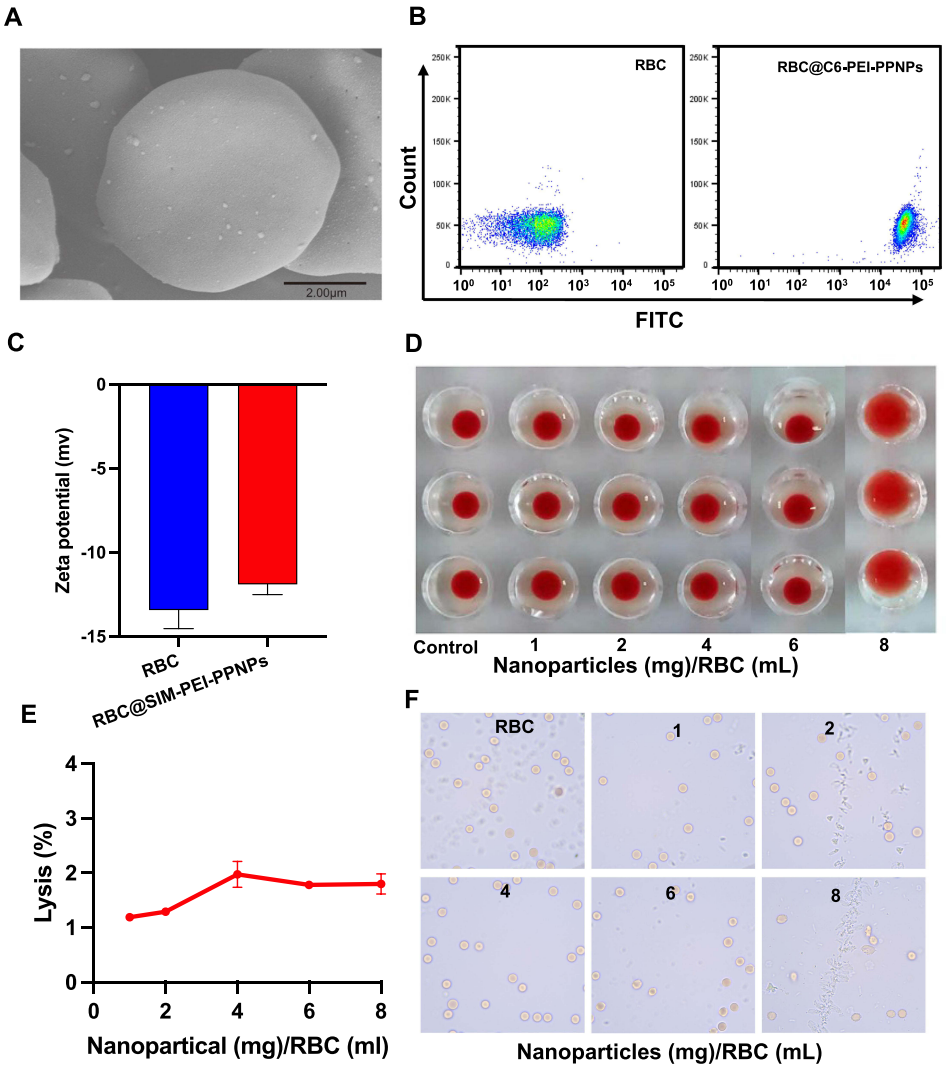

Figure 2 Characterization of RBC@SIM-PEI-PPNP and red blood cell-related toxicity studies. (**A**) Scanning electron microscope picture of RBC@SIM-PEI-PPNPs. Scare bar = 2 μm. (**B**) Quantitative results of nanoparticles adsorbed on RBC surface by flow cytometry. (**C**) Zeta potential of RBC and RBC@SIM-PEI-PPNPs. (**D**) Hemagglutination caused by SIM-PEI-PPNPs adhesion in U-shaped 96-well plates (n = 3). (**E**) Calculation of the percentage of erythrocyte lysis after incubation with SIM-PEI-PPNPs (n = 3). (**F**) Effect of SIM-PEI-PPNPs on RBC aggregation and morphology behavior.

As shown in Figure 2E, the relative hemolysis rate for the preparation of RBC@SIM-PEI-PPNPs with varying nanoparticle concentrations is consistently below the 5% hemolysis threshold set by international ASTM E2524-08 standards. This indicates that the addition of SIM-PEI-PPNPs has no significant impact on red blood cell hemolysis.[39]

To observe the morphology and aggregation of red blood cell carriers, different concentrations of SIM-PEI-PPNPs were added to blank red blood cells. Under an optical microscope, it was observed that, with increasing nanoparticle concentration, compared to normal red blood cells, the red blood cell carriers may undergo deformation. The experimental results in Figure 2F show that when the nanoparticle concentration exceeds 6 mg/mL, the red blood cell carriers experience deformation, likely due to the excessive adsorption of positively charged nanoparticles on the red blood cell surfaces, affecting the fluidity of the red blood cell membrane.[40]

Considering the comprehensive assessment of red blood cell-related toxicity studies, a SIM-PEI-PPNPs/RBC (w/v) concentration of 6 mg/mL was identified as the optimal concentration for preparing the red blood cell-loaded nanoparticle drug delivery system. Subsequent in vitro characterization and evaluation will be conducted at this concentration.

Evaluation of RBC@SIM-PEI-PPNPs in vitro

The osmotic fragility test is used to assess the ability of RBC to resist hemolysis induced by low salt solutions. The obtained osmotic fragility curves are shown in Figure 3A. The curves exhibit an overall sigmoid shape, with the hemolysis rate increasing as the NaCl solution concentration decreases. When the NaCl solution concentration was 0.55% (w/v), both blank-packed RBC and RBC@SIM-PEI-PPNPs began to experience cell lysis. At a NaCl solution concentration of 0.30% (w/v), both groups experience complete hemolysis. Furthermore, blank-packed RBC and RBC@SIM-PEI-PPNPs show similar osmotic fragility, indicating that the surface adsorption of nanoparticles has no significant impact on the osmotic fragility of RBC.

Turbulent fragility reflects the tolerance of RBC to hemolysis under mechanical stress induced by turbulence during blood circulation. The hemolysis rate of RBC is represented under certain shear conditions. A turbulent fragility curve was obtained by plotting the hemolysis rate against the shaking time on a constant-temperature shaker, as shown in Figure 3B. The results indicate that with an increase in shaking time, the hemolysis rate of RBC gradually rises, and turbulent fragility decreases. RBC and RBC@SIM-PEI-PPNPs have similar turbulent fragility at the same time, suggesting that the surface adhesion of nanoparticles has no significant effect on their turbulent fragility.

The results obtained from flow cytometry for FITC fluorescence intensity and the percentage of positive cells were shown in Figure 3C and D. The RBC@SIM-PEI-PPNPs group had a FITC-positive cell percentage of 2.55 ± 1.77%, which was not significantly different from the FITC-positive cell percentage of the RBC group (1.81 ± 0.30%) and much lower than that of the red blood cell control group (73.77 ± 1.60%). This suggests that both RBC and RBC@SIM-PEI-PPNPs have significantly lower phosphatidylserine exposure compared to the red blood cell control, indicating minimal red blood cell damage. These results demonstrate that the adsorption of positively charged nanoparticles to the red blood cell carrier causes minimal damage, which can be neglected.

SIM-PEI-PPNPs nonspecifically adhere to the red blood cell surface, and this adsorption process was reversible. In the bloodstream, nanoparticles adsorbed on the red blood cell surface may detach due to shear stress in the blood flow.

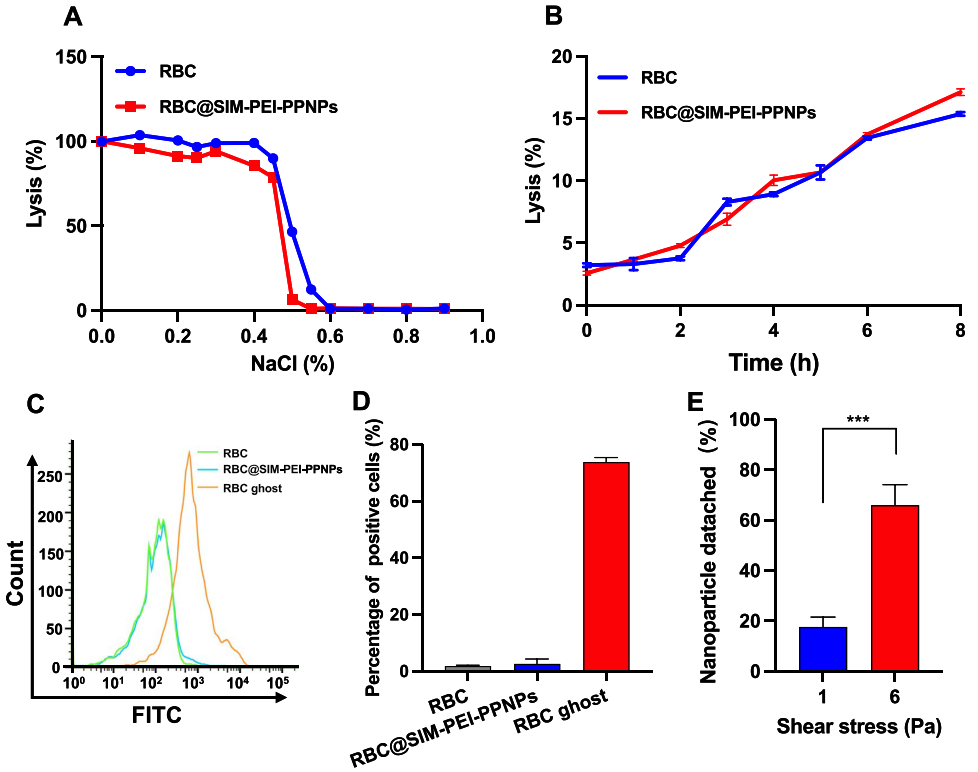

Figure 3 Evaluation of RBC@SIM-PEI-PPNPs in vitro. (**A**) Osmotic fragility curves of RBC and RBC@SIM-PEI-PPNPs (n = 3). (**B**) Turbulence fragility curves of RBC and RBC@SIM-PEI-PPNPs (n = 3). (**C**) FITC fluorescence intensity and (**D**) percentage of positive cells by flow cytometry (n = 3). (**E**) Percent nanoparticles detached from the carrier RBC under in vitro shear conditions (n = 3, ***p < 0.001).

The shear responsiveness of RBC@SIM-PEI-PPNPs in simulated body circulation (1 Pa) and lung capillaries (6 Pa) under different shear stresses was characterized using a microfluidic visual viscometer. The results in Figure 3E show that, compared to low shear stress, there is a significant increase in the detachment rate of nanoparticles from the red blood cell surface at high shear stress ($p<0.001$). At 1 Pa shear stress, only a small number of nanoparticles detach, whereas at 6 Pa shear stress, over 60% of the nanoparticles detach from the red blood cell surface. The experimental results indicate that RBC@SIM-PEI-PPNPs can exhibit shear responsiveness in the lungs, and maintain nanoparticle adhesion in low-shear stress environments in the systemic circulation, providing a degree of prolonged circulation. Simultaneously, they detach in the high-shear stress environment of lung capillaries, enabling nanoparticle lung-targeted delivery, facilitating drug accumulation in the lungs, and thus improving therapeutic efficacy.

Red Blood Cell Surface-Loaded Nanoparticle Intracellular Distribution Experiment

The lung-targeted distribution of the red blood cell surface-loaded nanoparticle drug delivery system in mice was evaluated through in vivo imaging experiments. Healthy ICR mice were separately administered DiR-PEI-PPNPs and RBC@DiR-PEI-PPNPs via tail vein injection. The in vivo imaging results at 0.5 h and 2 h after administration are presented in Figure 4A. Following the administration of DiR-PEI-PPNPs, these nanoparticles rapidly distributed in the liver region, likely due to the reticuloendothelial system (RES) clearance of nanoparticles in the mouse body. In contrast, at 0.5 h after administration, the fluorescence intensity in the lung region of mice treated with RBC@DiR-PEI -PPNPs was significantly higher than that in the DiR-PEI-PPNPs group. This indicates that, compared to free nanoparticles, the nanoparticle drug delivery system adhered to the surface of red blood cells rapidly increasing nanoparticle accumulation in the lung region after intravenous administration, achieving lung-targeting effects. After 2 h, the lung fluorescence intensity remained higher in the RBC@DiR-PEI-PPNPs group compared to the DiR-PEI-PPNPs group, indicating that RBC@DiR-PEI-PPNPs have a certain degree of lung-targeting capability and retention in the mouse body.

To further observe the distribution of nanoparticles in various tissues, ICR mice were administered DiR-PEI-PPNPs and RBC@DiR-PEI-PPNPs via tail vein injection, and at 0.5 h and 2 h after administration, the mice were euthanized, and various organ tissues and blood were collected. Organ observations were conducted using a small animal imaging system, and the fluorescence intensity in various organ tissues and blood was semi-quantitatively analyzed using Living Image 4.5 software, as shown in Figure 4B. After semi-quantitative analysis, as depicted in Figure 4C and D, at 0.5 h after administration, the lung fluorescence intensity in the RBC@DiR-PEI-PPNPs group was significantly higher than in the DiR-PEI-PPNPs group ($p<0.01$), and the blood fluorescence intensity in the RBC@DiR-PEI-PPNPs group was higher than in the DiR-PEI-PPNPs group. This indicates that adsorbing nanoparticles on the surface of red blood cells can prevent them from being engulfed by the RES system while promoting their accumulation in the lungs. After 2 h of administration, both the lung and blood fluorescence intensity in the RBC@DiR-PEI-PPNPs group remained significantly higher than in the DiR-PEI-PPNPs group ($p<0.05$). In summary, free nanoparticles, when administered via intravenous injection, are quickly metabolized in the liver, resulting in relatively low lung distribution. Conversely, adsorbing them onto red blood cells can prolong their circulation time in the body and enhance their lung accumulation.

In the Context of Animal Pharmacological Studies Involving Red Blood Cell Surface-Loaded Nanoparticles

The lung wet-to-dry weight ratio (W/D) represents lung tissue water content and serves as a direct indicator of pulmonary edema, which results from significant fluid leakage into the alveoli and lung interstitium following tracheal instillation of LPS, leading to an increase in lung wet weight while lung dry weight remains unaffected. Typically, the impact of drugs on lung edema in ARDS mice is evaluated by measuring the ratio of lung wet weight to dry weight. As depicted in Figure 5A, compared to the Control group, the lung W/D value significantly increased in mice after LPS stimulation ($p<0.0001$), indicating a pronounced lung edema pathology triggered by intratracheal LPS instillation. In contrast, the lung W/D value in the RBC@SIM-PEI-PPNPs group significantly decreased compared to the ARDS model group ($p<0.01$), suggesting that it can mitigate the symptoms of lung edema in ARDS model mice.

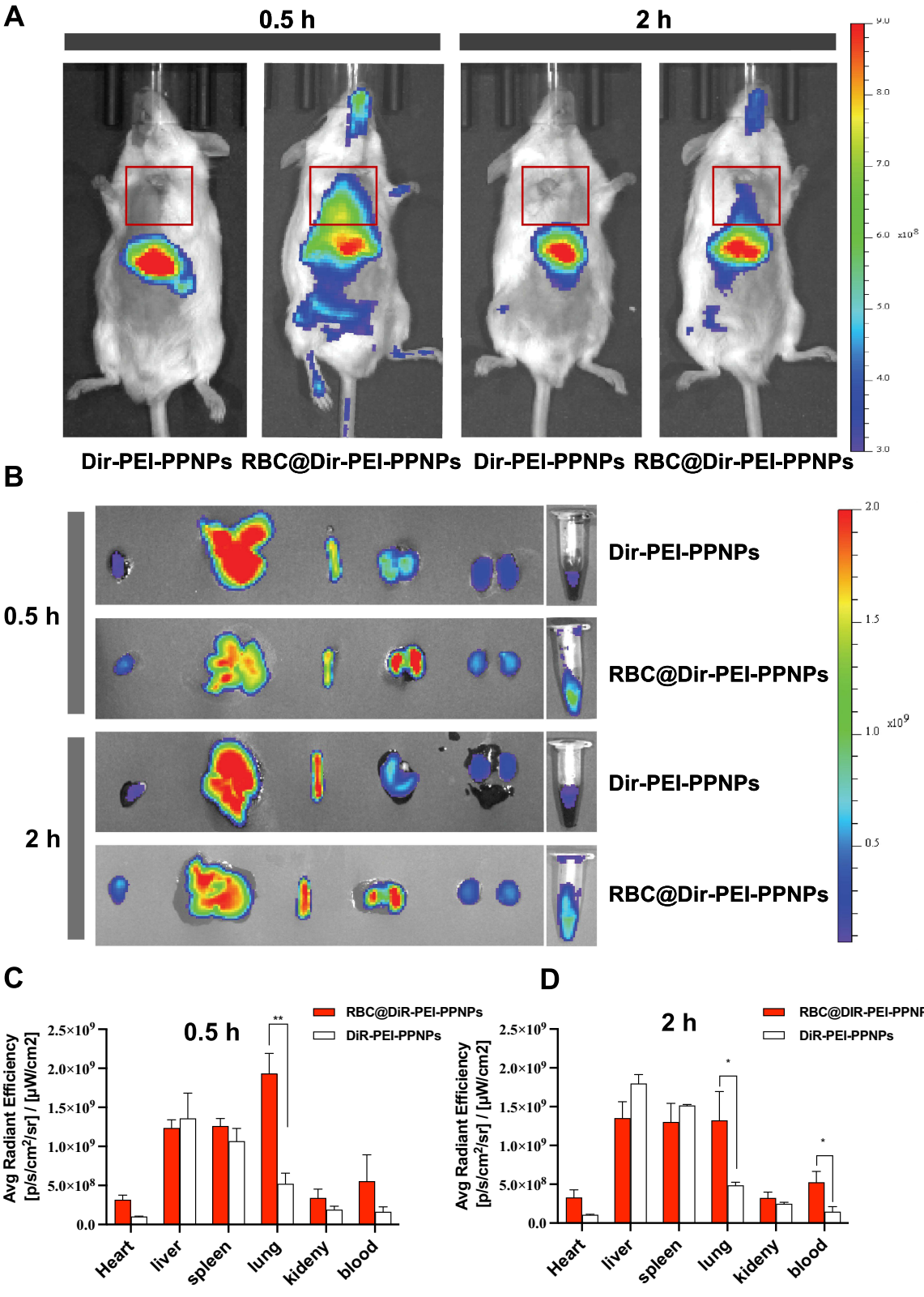

Figure 4 Biodistribution of RBC@DiR-PEI-PPNPs in vivo. (**A**) Biodistribution of DiR-PEI-PPNPs and RBC@DiR-PEI-PPNPs in vivo at 0.5 h and 2 h, the solid red box represents the area where the lung tissue is located (n = 3). (**B**) The fluorescence images of excised representative organs from mice. (**C**) The semi-quantified fluorescence intensity in the representative organs, expressed as the average fluorescence intensity in 0.5 h and (**D**) 2 h (Avg Radiant Efficiency, n = 3, *p < 0.05, **p < 0.01).

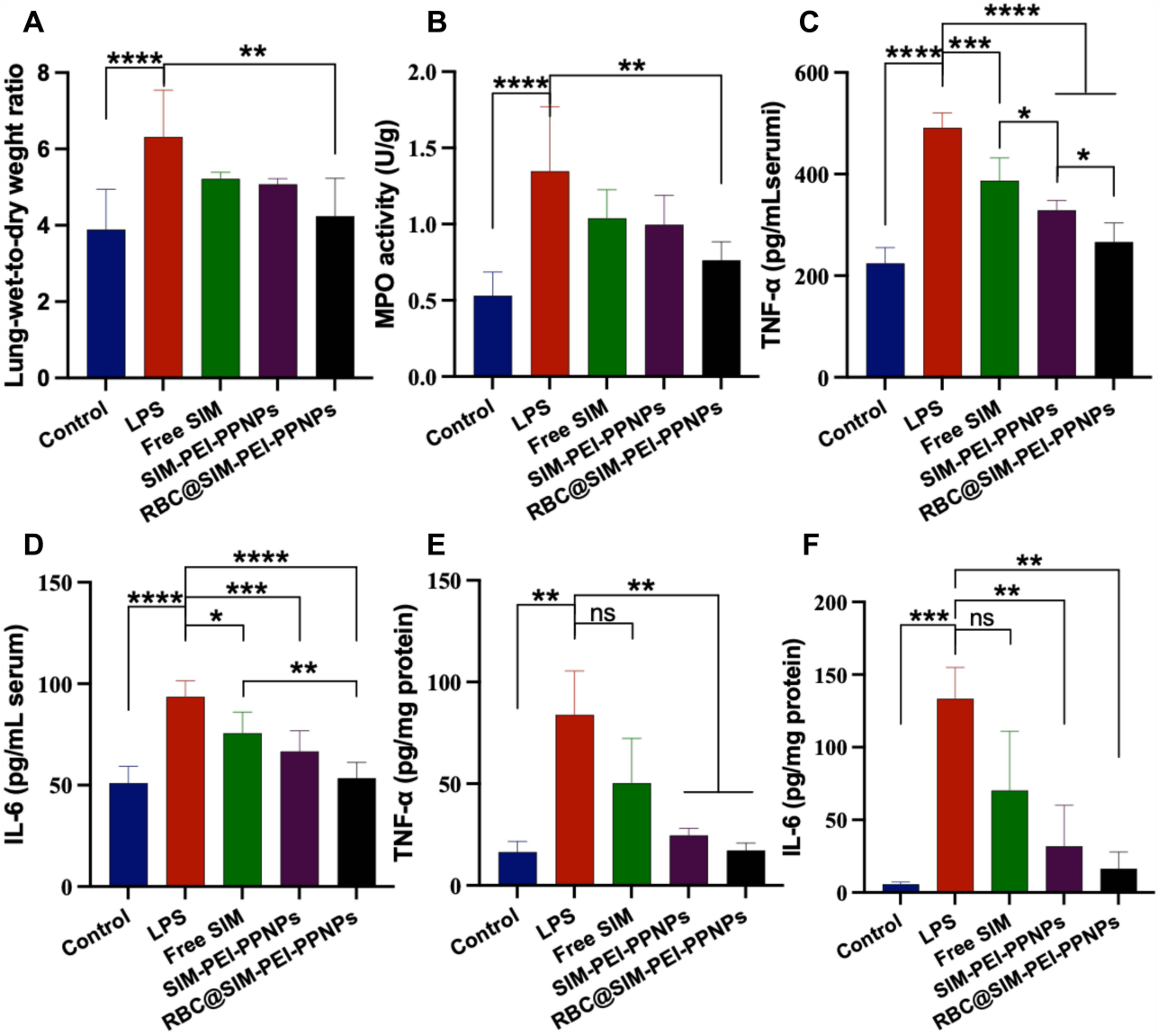

Figure 5 Determination of lung tissue and serum related indexes. (**A**) The wet/dry weight ratio of lung tissue in ICR mice was 24 h after administration (n = 6, **p < 0.01, ****p < 0.0001). (**B**) The MPO activity of lung tissue in ICR mice was 24 h after administration (n = 6, **p < 0.01, ****p < 0.0001). (**C**) The level of inflammatory cytokines in serum of ICR mice was 24 h after administration TNF-α level. (**D**) IL-6 level (n = 6, *p < 0.05, **p < 0.01, ***p < 0.001, ****p < 0.0001). (**E**) The level of inflammatory cytokines in lung tissue of ICR mice was 24 h after administration TNF-α level (**F**) IL-6 level (n = 3, **p < 0.01, ***p < 0.001).

MPO, an enzyme relatively stable in neutrophils, serves as an indicator of neutrophil accumulation in inflammatory tissues. Measuring MPO activity in lung tissue homogenates can further verify changes in neutrophil quantity in inflammatory tissues. A significant infiltration of neutrophils into lung tissues can lead to lung damage. As shown in Figure 5B, the LPS group exhibited significantly increased MPO activity compared to the Control group ($p<0.0001$), confirming the successful establishment of the ARDS mouse model. MPO activity was reduced in the free SIM group, SIM-PEI-PPNPs group, and RBC@SIM-PEI-PPNPs group compared to the LPS group, with the RBC@SIM-PEI-PPNPs group showing a significant reduction in MPO activity ($p<0.01$). This indicates that RBC@SIM-PEI-PPNPs have a more pronounced effect in lowering MPO activity in lung tissues and suppressing neutrophil infiltration, thus alleviating the inflammatory response in ARDS.

Blood serum was collected from mice 24 h after drug administration, and ELISA kits were used to measure TNF-α and IL-6 levels. The results are presented in Figure 5C and D. Compared to the control group, the LPS group showed a significant increase in serum TNF-α and IL-6 levels ($p<0.0001$), indicating a systemic inflammatory response induced

by intratracheal LPS in the ARDS model group. After treatment with drugs and drug carriers, all groups of mice exhibited varying degrees of reduction in serum TNF-α and IL-6 levels, all with statistical significance. This suggests that the drugs in each group effectively improved the systemic inflammatory response caused by LPS-induced ARDS. In comparison to the LPS group, the free SIM group, SIM-PEI-PPNPs group, and RBC@SIM-PEI-PPNPs group all reduced serum IL-6 and TNF-α levels. Among the treatment groups, the RBC@SIM-PEI-PPNPs group demonstrated a stronger effect in suppressing serum TNF-α and IL-6 levels 24 h after administration, indicating that red blood cell surface-loaded nanoparticles have a more potent role in inhibiting the production of inflammatory factors in ARDS. To further demonstrate the targeted effect of the formulation, we investigated the inflammation of lung tissue in different groups of mice. As shown in Figure 5E and F, the overall trend was consistent with the inflammatory indicators in serum, and the results showed that RBC@SIM-PEI-PPNPs had a better therapeutic effect compared with other treatment groups, indicating that the accumulation of RBC@SIM-PEI-PPNPs in lung tissue was more, and further indirectly indicated that RBC@SIM-PEI-PPNPs had a certain degree of lung tissue targeting.

Pathological Changes in Lung Tissue

After 24 h of drug administration, lung tissues from each group of mice were subjected to HE staining, and pathological sections were prepared. These sections were observed under an optical microscope to assess the improvement in lung tissue pathology relative to the ARDS model in mice treated with free SIM, SIM-PEI-PPNPs, and RBC@SIM-PEI-PPNPs. The experimental results, as shown in Figure 6, reveal the following: In the control group, the lung tissue structure was clear and intact, with no thickening of alveolar walls, relatively consistent alveolar size, and no signs of inflammatory cell infiltration. In the LPS group, the lung tissue pathological sections displayed severe inflammatory reactions, including inflammatory cell infiltration, edema and thickening of alveolar septa, collapse of alveolar structure, and intrapulmonary bleeding. The intervention groups with free SIM, SIM-PEI-PPNPs, and RBC@SIM-PEI-PPNPs exhibited varying degrees of improvement in the pathological features of lung tissue inflammation in comparison to the ARDS model group. Among them, the RBC@SIM-PEI-PPNPs group demonstrated the most significant improvement in lung tissue pathology, with reduced inflammatory cell infiltration, thickening of alveolar septa, and lung tissue congestion, compared to the groups treated with free SIM and SIM-PEI-PPNPs. This indicates that RBC@SIM-PEI-PPNPs

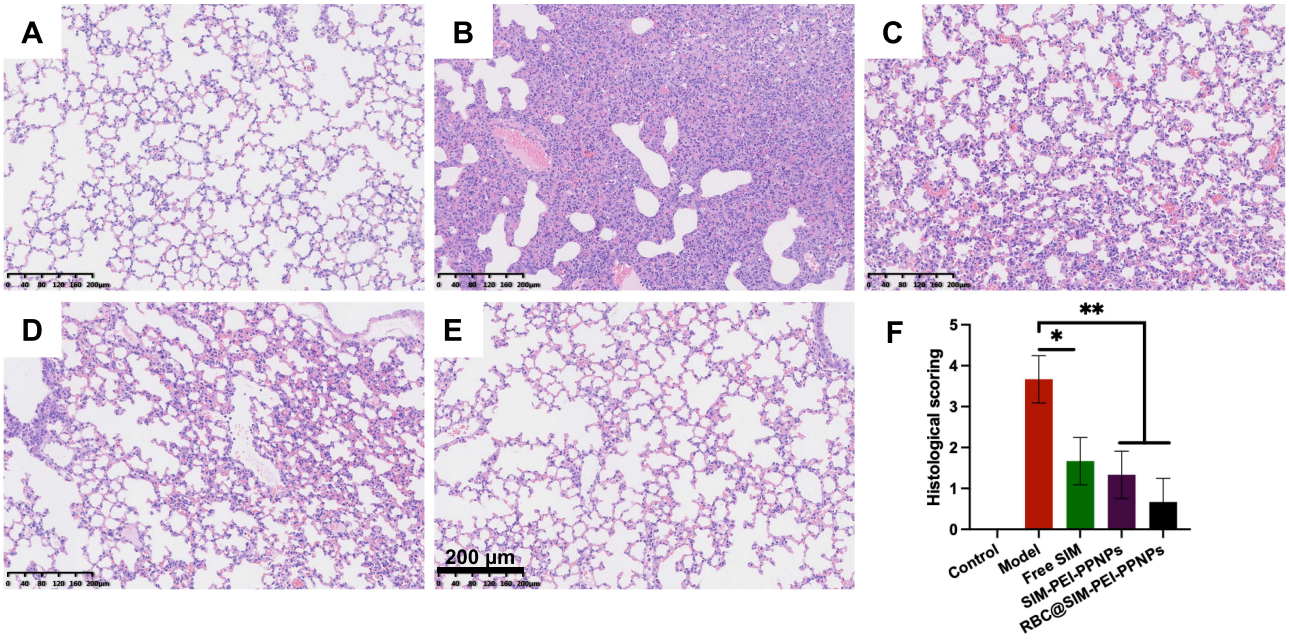

Figure 6 Histopathological examination. Lung section of (**A**) Control mice, (**B**) LPS-induced model mice, (**C**) Free simvastatin treated mice, (**D**) SIM-PEI-PPNPs treated mice. (**E**) RBC@SIM-PEI-PPNPs treated mice. Scare bar = 200 μm. (**F**) Histological evaluation scores of H&E staining in the lungs of mice in different groups (n = 3, *p<0.05, **p < 0.01).

have the strongest effect in alleviating lung inflammation and pathological damage in ARDS mice. Then, we scored the morphology of lung tissues in different groups of mice, and the evaluation indicators are shown in Table 1. The pulmonary histology evaluation score was shown in Figure 6F, this result further indicates that RBC@SIM-PEI-PPNPs have the best therapeutic effect on reducing lung inflammation.

Discussion

Incorporating a delivery system that combines nanotechnology and cellular carriers can effectively extend the drug's circulation time in the body and enhance targeted distribution in the lungs. Therefore, this study holds significant research value and application potential. Using SIM as a model drug, this study employs RBC surface-loading nanoparticle drug delivery strategy. The pH-responsive cationic nanoparticles loaded with SIM are non-covalently adsorbed onto the RBC surface to create a nanoparticle-based RBC surface drug delivery system. This approach extends the drug's circulation time, promotes effective accumulation in the lungs, improves drug efficacy, and reduces side effects. However, further investigation is still needed.

The cationic PEI was modified on the nanoparticle surface to load SIM, allowing adsorption onto the negatively charged RBC surface through electrostatic interactions. This process created an RBC surface-loaded cationic pH-responsive PLGA nanoparticle delivery system. Characterization of the formulation and in vitro release studies under varying pH conditions confirmed the pH-responsive nature of the system. When SIM-PEI-PPNPs attached to the RBC surface, the RBC's negative charge decreased, indicating successful adsorption through electrostatic interactions. Subsequent in vivo and in vitro evaluations verified the therapeutic efficacy of the system.

The strong lung-targeting capability of RBC@SIM-PEI-PPNPs likely enables higher drug concentrations in the lungs for anti-inflammatory effects. Intravenous injection of RBC@SIM-PEI-PPNPs in ARDS mice revealed that the red blood cell surface-adsorbed drug delivery system dislodges from the RBC surface in the high-shear environment of narrow lung capillaries, releasing SIM-PEI-PPNPs to accumulate in the pulmonary capillary endothelium. This process effectively targets the lungs. Additionally, the acidic microenvironment at the ARDS site promotes acid-responsive drug release from SIM-PEI-PPNPs, enhancing effective delivery of SIM to the lung lesion site. Consequently, compared to free drugs and drug-loaded nanoparticles, RBC@SIM-PEI-PPNPs demonstrate more potent therapeutic effects in ARDS mice. The lung tissue histology aligns with changes in lung tissue MPO activity and inflammatory factor levels. This outcome is likely due to the strong lung-targeting capability of RBC@SIM-PEI-PPNPs, enabling delivery of higher drug concentrations to the lungs for anti-inflammatory effects.

Although this study used in vivo imaging in mice to investigate the targeting and long-circulation characteristics of the RBC surface-loaded nanoparticles, the retention time of nanoparticles in the lungs and blood was not thoroughly examined. Future research could extend the imaging duration in small animals to explore the retention time of nanoparticles in the lungs. Additionally, in vivo pharmacokinetic studies of RBC@SIM-PEI-PPNPs could further assess the formulation's long-circulation effect. Further investigation into the fate of red blood cells as drug delivery carriers' post-intravenous injection is needed, which could be accomplished using flow cytometry to measure the lifespan of biotin-labeled RBCs in vivo.

Conclusion

In this study, to address the poor water solubility of SIM, PLGA was used to encapsulate SIM to improve the solubility and bioavailability. Leveraging the slightly acidic environment of the Inflammatory Microenvironment (IME) in ARDS lung tissue lesions, a pH-responsive factor, $NaHCO_3$, was co-encapsulated with SIM within the PLGA nanoparticles, rendering them pH-responsive for rapid drug release at the site of lung tissue lesions in the IME. By modifying the nanoparticle surface with the cationic agent, PEI, cationic pH-responsive PLGA nanoparticles loaded with SIM were created. These nanoparticles can adsorb onto negatively charged red blood cell surfaces through electrostatic interactions, leading to the development of red blood cell-surface-loaded cationic pH-responsive PLGA nanoparticle drug delivery system. Through shear-responsive actions, the nanoparticles are targeted for delivery to the lungs and, in the slightly acidic environment of the IME at the site of ARDS lesions, release the drug responsively. This system exhibits a strong capacity to ameliorate early-stage lung edema, inflammatory cell infiltration, cytokine production, and lung tissue pathology in ARDS mice, offering a novel approach to the safe and effective treatment of ARDS.

Acknowledgments

This work was supported by a grant from the National Natural Science Foundation of China (81600061) and Nanjing Medical Science and Technique Development Foundation (Young Talent Project QRX17077).

Disclosure

The authors report no conflicts of interest in this work.

References

1. Meyer NJ, Gattinoni L, Calfee CS. Acute respiratory distress syndrome. *Lancet*. 2021;398(10300):622–637. doi:10.1016/s0140-6736(21)00439-6
2. Bos LDJ, Ware LB. Acute respiratory distress syndrome: causes, pathophysiology, and phenotypes. *Lancet*. 2022;400(10358):1145–1156. doi:10.1016/s0140-6736(22)01485-4
3. Chen J, Ma S, Luo B, et al. Human umbilical cord mesenchymal stromal cell small extracellular vesicle transfer of microRNA-223-3p to lung epithelial cells attenuates inflammation in acute lung injury in mice. *J Nanobiotechnology*. 2023;21(1):295. doi:10.1186/s12951-023-02038-3
4. Kellner M, Noonepalle S, Lu Q, Srivastava A, Zemskov E, Black SM. ROS signaling in the pathogenesis of Acute Lung Injury (ALI) and Acute Respiratory Distress Syndrome (ARDS). *Adv Exp Med Biol*. 2017;967:105–137. doi:10.1007/978-3-319-63245-2_8
5. Potey PM, Rossi AG, Lucas CD, Dorward DA. Neutrophils in the initiation and resolution of acute pulmonary inflammation: understanding biological function and therapeutic potential. *J Pathol Apr*. 2019;247(5):672–685. doi:10.1002/path.5221
6. Andreakos E, Papadaki M, Serhan CN. Dexamethasone, pro-resolving lipid mediators and resolution of inflammation in COVID-19. *Allergy*. 2021;76(3):626–628. doi:10.1111/all.14595
7. Villar J, Ferrando C, Martínez D, et al. Dexamethasone treatment for the acute respiratory distress syndrome: a multicentre, randomised controlled trial. *Lancet Respir Med*. 2020;8(3):267–276. doi:10.1016/s2213-2600(19)30417-5
8. Steinberg KP, Hudson LD, Goodman RB, et al. Efficacy and safety of corticosteroids for persistent acute respiratory distress syndrome. *N Engl J Med*. 2006;354(16):1671–1684. doi:10.1056/NEJMoa051693
9. Li D, Wang X, Liao Y, Wang S, Shan J, Ji J. Insights gained into the treatment of COVID19 by pulmonary surfactant and its components. *Front Immunol*. 2022;13:842453. doi:10.3389/fimmu.2022.842453
10. Choi JS, Lee HS, Seo KH, et al. The effect of post-treatment N-acetylcysteine in LPS-induced acute lung injury of rats. *Tuberc Respir Dis*. 2012;73(1):22–31. doi:10.4046/trd.2012.73.1.22
11. Rendell R, Fairhall S, Graham S, et al. Assessment of N-acetylcysteine as a therapy for phosgene-induced acute lung injury. *Toxicol Lett*. 2018;290:145–152. doi:10.1016/j.toxlet.2018.03.025
12. Deponte M. Glutathione catalysis and the reaction mechanisms of glutathione-dependent enzymes. *Biochim Biophys Acta*. 2013;1830(5):3217–3266. doi:10.1016/j.bbagen.2012.09.018
13. Bao XC, Mao AR, Fang YQ, et al. Simvastatin decreases hyperbaric oxygen-induced acute lung injury by upregulating eNOS. *Am J Physiol Lung Cell Mol Physiol*. 2018;314(2):L287–l297. doi:10.1152/ajplung.00520.2016
14. Tleyjeh IM, Kashour T, Hakim FA, et al. Statins for the prevention and treatment of infections: a systematic review and meta-analysis. *Arch Intern Med*. 2009;169(18):1658–1667. doi:10.1001/archinternmed.2009.286
15. Xiong B, Wang C, Tan J, et al. Statins for the prevention and treatment of acute lung injury and acute respiratory distress syndrome: a systematic review and meta-analysis. *Respirology*. 2016;21(6):1026–1033. doi:10.1111/resp.12820
16. Aikawa N, Ishizaka A, Hirasawa H, et al. Reevaluation of the efficacy and safety of the neutrophil elastase inhibitor, Sivelestat, for the treatment of acute lung injury associated with systemic inflammatory response syndrome; a Phase IV study. *Pulm Pharmacol Ther*. 2011;24(5):549–554. doi:10.1016/j.pupt.2011.03.001
17. Marchetti C, Swartzwelter B, Gamboni F, et al. OLT1177, a β-sulfonyl nitrile compound, safe in humans, inhibits the NLRP3 inflammasome and reverses the metabolic cost of inflammation. *Proc Natl Acad Sci U S A*. 2018;115(7):E1530–e1539. doi:10.1073/pnas.1716095115
18. Zeiher BG, Artigas A, Vincent JL, et al. Neutrophil elastase inhibition in acute lung injury: results of the STRIVE study. *Crit Care Med*. 2004;32(8):1695–1702. doi:10.1097/01.ccm.0000133332.48386.85
19. Matthay MA, Zemans RL, Zimmerman GA, et al. Acute respiratory distress syndrome. *Nat Rev Dis Primers*. 2019;5(1):18. doi:10.1038/s41572-019-0069-0
20. Zhang J, Huang X, Ding D, et al. Comparative Study of Acute Lung Injury in COVID-19 and Non-COVID-19 Patients. *Front Med Lausanne*. 2021;8:666629. doi:10.3389/fmed.2021.666629
21. Bellani G, Laffey JG, Pham T, et al. Epidemiology, patterns of care, and mortality for patients with acute respiratory distress syndrome in intensive care units in 50 countries. *JAMA*. 2016;315(8):788–800. doi:10.1001/jama.2016.0291
22. Estanislau IM, Terceiro IR, Lisboa MR, et al. Pleiotropic effects of statins on the treatment of chronic periodontitis--a systematic review. *Br J Clin Pharmacol*. 2015;79(6):877–885. doi:10.1111/bcp.12564
23. Sakoda K, Yamamoto M, Negishi Y, Liao JK, Node K, Izumi Y. Simvastatin decreases IL-6 and IL-8 production in epithelial cells. *J Dent Res*. 2006;85(6):520–523. doi:10.1177/154405910608500608
24. Zeiser R. Immune modulatory effects of statins. *Immunology*. 2018;154(1):69–75. doi:10.1111/imm.12902
25. Altwairgi AK. Statins are potential anticancerous agents (review). *Oncol Rep*. 2015;33(3):1019–1039. doi:10.3892/or.2015.3741
26. Borgquist S, Bjarnadottir O, Kimbung S, Ahern TP. Statins: a role in breast cancer therapy? *J Intern Med*. 2018;284(4):346–357. doi:10.1111/joim.12806
27. Kong R, Zhu X, Meteleva ES, et al. Enhanced solubility and bioavailability of simvastatin by mechanochemically obtained complexes. *Int J Pharm*. 2017;534(1–2):108–118. doi:10.1016/j.ijpharm.2017.10.011
28. Fang RH, Kroll AV, Gao W, Zhang L. Cell membrane coating nanotechnology. *Adv Mater*. 2018;30(23):e1706759. doi:10.1002/adma.201706759
29. Cheng Z, Liu S, Wu X, et al. Autologous erythrocytes delivery of berberine hydrochloride with long-acting effect for hypolipidemia treatment. *Drug Deliv*. 2020;27(1):283–291. doi:10.1080/10717544.2020.1716880

30. Sahoo K, Koralege RS, Flynn N, et al. Nanoparticle attachment to erythrocyte via the glycophorin a targeted ERY1 ligand enhances binding without impacting cellular function. *Pharm Res*. 2016;33(5):1191–1203. doi:10.1007/s11095-016-1864-x
31. Antonelli A, Sfara C, Weber O, et al. Characterization of ferucarbotran-loaded RBCs as long circulating magnetic contrast agents. *Nanomedicine (London, England)*. 2016;11(21):2781–2795. doi:10.2217/nnm-2016-0216 *Nanomedicine (Lond)*.
32. Antonelli A, Pacifico S, Sfara C, Tamma M, Magnani M. Ferucarbotran-loaded red blood cells as long circulating MRI contrast agents: first in vivo results in mice. *Nanomedicine (London, England)*. 2018;13(7):675–687. doi:10.2217/nnm-2017-0339 *Nanomedicine (Lond)*.
33. Ma Q, Fan Q, Xu J, et al. Calming cytokine storm in pneumonia by targeted delivery of TPCA-1 using platelet-derived extracellular vesicles. *Matter*. 2020;3(1):287–301. doi:10.1016/j.matt.2020.05.017
34. Zhang CY, Lin W, Gao J, et al. pH-responsive nanoparticles targeted to lungs for improved therapy of acute lung inflammation/injury. *ACS Appl Mater Interfaces*. 2019;11(18):16380–16390. doi:10.1021/acsami.9b04051
35. Goodhead LK, MacMillan FM. Measuring osmosis and hemolysis of red blood cells. *Adv Physiol Educ*. 2017;41(2):298–305. doi:10.1152/advan.00083.2016
36. Pulliam KE, Joseph B, Makley AT, et al. Washing packed red blood cells decreases red blood cell storage lesion formation. *Surgery*. 2021;169(3):666–670. doi:10.1016/j.surg.2020.07.022
37. Zhao Z, Ukidve A, Krishnan V, et al. Systemic tumour suppression via the preferential accumulation of erythrocyte-anchored chemokine-encapsulating nanoparticles in lung metastases. *Nat Biomed Eng*. 2021;5(5):441–454. doi:10.1038/s41551-020-00644-2
38. Lei J, Wang L, Zou L, et al. GDF3 protects mice against sepsis-induced acute lung injury by suppression of macrophage pyroptosis. *Pharmaceuticals*. 2024;17(3):268. doi:10.3390/ph17030268
39. Slowing W, CW Vivero-Escoto JL, Lin VS, Lin VS-Y. Mesoporous silica nanoparticles for reducing hemolytic activity towards mammalian red blood cells. *Small*. 2009;5(1):57–62. doi:10.1002/smll.200800926
40. Karabasz A, Szczepanowicz K, Cierniak A, Bereta J, Bzowska M. In vitro toxicity studies of biodegradable, polyelectrolyte nanocapsules. *Int J Nanomed*. 2018;13:5159–5172. doi:10.2147/ijn.S169120